CGU HS Committee on River Ice Processes and the Environment
15th Workshop on River Ice
St. John's, Newfoundland and Labrador, June 15 - 17, 2009

Frazil ice as a geomorphic agent

Geneviève Allard[1], Thomas Buffin-Bélanger[1] and Normand Bergeron[2]
1. Université du Québec à Rimouski, Département de biologie, de chimie et de géographie, 300, allée des Ursulines, Rimouski, (Québec), G5L 3A1, Canada.
2. Institut national de la recherche scientifique - Centre Eau, Terre et Environnement, Université du Québec, 490, rue de la Couronne, Québec (Québec), G1K 9A9, Canada.
Email adresses genallard@yahoo.ca; thomas_buffin-belanger@uqar.qc.ca; Normand.Bergeron@ete.inrs.ca

This paper addresses the bidirectional linkages between frazil ice dynamics and alluvial bedforms. Frazil forms in open water area of high turbulent intensity and accumulates downstream along flatter river segments. The activation of production zones, in relation to hydroclimatic parameters, directly affects the infilling of frazil sinks (accumulation zones). Past field investigations have described strong relationships between riverbed scour and undercover frazil accumulation but few have documented the dynamics of bed changes in relation to the accumulation of frazil ice over an entire winter season.

Here, we present the chronology of an undercover frazil accumulation event at a pool section during the 2007-2008 ice period. The characteristics of upstream frazil ice production, ice cover growth, undercover frazil ice accumulation behavior, water level variation, hydroclimatic conditions and riverbed deformations are described. Bathymetric surveys were conducted before and after the winter season to compare the bed morphologies. During the ice period, innovative *dynamic bed-rods* integrating three-axis accelerometer pendant loggers were strategically deployed at the bed to obtain a dynamic measurement of erosional or depositional activity over the pool section. Data shows that most bedform changes relate to specific events. Ground penetrating radar and manual sounding investigations were conducted on a monthly basis. Analysis reveals the physical attributes of ice cover, undercover frazil accumulation and bedforms. Collected data is used to evaluate riverbed deformation's relation to iceforms.

1. Introduction

Ice processes occur in 60 % of major basins in the northern hemisphere and frazil ice is one of the key processes contributing to fluvial dynamics (Fig. 1). Frazil ice forms in open water area of high turbulent intensity and accumulates downstream along flatter river segments. The activation of production zones, in relation to hydroclimatic parameters, directly affects the infilling of ice covered *frazil sinks* such as deep pools, meanders and lake inflows. Numerous studies have investigated the large localized deposits of river ice known as hanging dam and it is well known that scour can be found beneath an ice jam. However, few studies have documented riverbed alteration in relation to the accumulation of frazil ice. Sui *et al.* (2000) proposed a conceptual empirical relation between hydraulics, frazil jam thickness and riverbed deformation. In 2006, Sui *et al.* showed a clear relationship between bed scour and ice accumulation within a single cross-section. Ettema (2002) suggested that temporal responses, such as channel readjustment to ice accumulation may have surprising enduring impacts.

This study presents the chronology of channel adjustments in relation to frazil ice accumulation within seven cross-sections at a pool section during the 2007-2008 ice period. This research was conducted with the following objectives in mind:

1. to obtain a better understanding of the infilling dynamics of frazil sinks.
2. to document the intensity and spatiality of channel response to specific events.
3. to investigate the evolution of the physical attributes of ice cover, undercover frazil accumulation and bed morphology on a monthly basis during a winter season.

2. Study Location

The Mitis River flows from the Appalachian plateau to the Saint-Lawrence maritime estuary. The Mitis River basin encompasses 1805 km², with an average elevation of 342 m. It has a length of 51 km from headwater reservoir Lac Mitis to Mitis Baie. The main tributaries are the Mistigougèche (82.3 km) and the Neigette rivers (117.1 km). The flow regime of the Mitis River is nivo-pluvial with highest discharges occurring in mid-May. Mean annual discharge of 33.3 m²/s (1921-1984), is submitted to upstream control from the retaining structures Mitis and Mistigougèche. Run-off-the river generating stations, Mitis-1 and 2 are implanted respectively at 1.8 and 2.6 km from estuary. The backflow of water from Mitis-2 dam is estimated to be 2 km long.

Data on freeze-up processes and ice cover progression were collected along a 23.8 km river corridor (Fig. 2). From PK36 to PK12.2, the river changes from a cobble and gravel bed riffle-pool sequence to a meandering planform downstream from Sainte-Angèle-de-Mérici. Average pool depth at low flow is 1.8 m (excluding pool PK14.1) and average width is 38 m for the riffle-pool section. Because of its intriguing higher depth, the meander pool PK14.1 was investigated for frazil accumulation and riverbed deformation (Fig. 2b, 3). The meander bend is fairly sharp with a deep pool towards the right bank. The 11 650 m² pool is composed of five (5) morphological units: (1) a cobble bed entrance slope; (2) the pool-center with a maximum bankfull flow depth of 8.2 m. Main channel bed is cobble and gravel throughout, but most of the bed within the secondary flow separation zone is sand; (3) a 75 meter long, ±3.5 m high (from channel bed) clay cliff constriction along entrance-slope to pool-center. The cliff is cut into Goldthwait Sea blue-gray marine clay underling Mitis terrace's silty intertidal deposits; (4) an

outer bank recirculation plateau composed of sand-gravel alluvial deposits overlying Mitis terrace's silt deposits; (5) a wide pool exit-slope with strong diverging flows.

3. Methods

Methods are detailed in table 1 and summarized below.

A freeze-up survey of visual on-site observations of frazil fed ice runs was documented at 27 survey sites on 21 visits. Four types of frazil fed ice-forms were documented: frazil fragments, ice aggregates, anchored ice and ice cover. The pool section was permanently monitored by a digital camera taking pictures at 10 minutes intervals.

Hydroclimatic data clarifies the influence of hydraulic and climatic factors associated with freeze-up conditions. Air and water temperature were measured at stations 4, 10 and 22. Water temperature and water level fluctuations were acquired at the pool section. Two water level loggers were deployed to document jam's backflow effect. Undercover flow measurements were unsuccessful due to frazil layer thickness.

Innovative *dynamic bed-rods* (DBR) were deployed at nine locations to measure scour and fill activity over the winter period. DBR are oversized bed pins vertically equipped three-axis accelerometer G-Pendant loggers evenly distributed on the rod. In-ground sensors are buried to expected scour depth and in-flow sensors emerge to expected fill height. Acceleration data is recorded in an internal memory for yearly download. A 70 min. sampling interval was chosen. Acceleration data was converted into a binary time series by using a 5 lags moving windows to obtain a RMS time series and applying a 0.3 threshold to that RMS series. This was done for both X and Y acceleration axis and resulted in a motion, no-motion time series. This method allows a "profiling" of the bed surface at all time. The DBR's height above bed was noted on installation and removal as another mean to measure erosion or deposition. At the same time, bed samples were taken. DBR 9 was not retrieved because it was buried under a pile of debris.

Ice and frazil layer physical attributes were documented using two methods: (1) direct drilling method and (2) indirect ground penetrating radar (GPR) investigations. GPR data was collected at pool site on January 29th. Two separate antenna arrangements were towed at constant speed over the ice cover following seven cross-sections. The 400 MHz antenna was used to detect frazil-water and water-bed interfaces and the 900 MHz antenna to detect the snow-ice layer thickness. Drill-hole measurements were made on February 29th and March 11th. Thickness measurement was taken in the drill-hole using a rigid graduated J-rod. The J-rod was lowered through the hole to bottom ice layer or until frazil-water density change was felt by the operator.

GPR data analysis for frazil ice detection is a three steps process. First, the original GPR image undergoes a filtering procedure to enhance the desired interfaces. In this study, a sequences of FIR wavenumber HP filters, FIR frequency LP filters and discrete wavelet transformations were used. Secondly, the enhanced layer profile is extracted from the image matrix. Using ArcGIS, the filtered matrix was converted to a 1x1 cell raster image. The interpretable interfaces were hand-drawn over the raster-image and corresponding raster coordinates were extracted. Thirdly, the extracted profiles are transformed into real measurements. X-values are converted in surveyed distances and Z-values are calibrated with drill-hole measurements. Calibration measurements confirmed a signal speed of 17cm/ns in snow-ice layer, 5.5 cm/ns in medium

dense frazil and 3.3 cm/ns in water. Of the difficulties encountered, one was that the antennas were unfit to probe an ice-frazil thickness greater than 4 meters. Another difficulty was that GPR signal analysis showed no results for 60% of the calibration holes. Vertical measurement errors are explained with result figure 6.

4. Results

Freeze-up dynamics along the river corridor

Figures 4 and 5 illustrate the spatio-temporal dynamic of river ice formation and the fluctuation of hydroclimatic parameters for the winter 2007-2008. First, frazil ice runs were observed at pool section from Nov. 23rd to Jan. 25th. The beginning of frazil ice formation is associated with a 0.8°C water temperature, a -4°C regional air temperature and -5°C FDD. Similar conditions were met on 11/12 and 11/20 but 11/23 differs with cooling daily temperatures. Major frazil factories are large rapids, elongated riffles, and the Mistigougèche tributary. The Neigette tributary, smaller tributaries and the 1m concrete dam waterfall at PK 36 had negligible production capacity. Cold periods (C) favors anchor ice growth, an indicator of frazil formation in local riffles. Factories activations migrated upstream as the warm reservoir water's cooled downstream. This is illustrated by the thermal gradient of water temperature.

Secondly, the upriver progression of a juxtaposed ice cover is controlled by both the hydroclimatic conditions and the river gradient. The ice cover's migrating speed varied significantly during progression: 203 m/day from PK5 to PK9, to 100 m/day between PK9 and PK14 and to 31 m/day between PK14 and PK19. The 5.8 km segment from PK19 to PK36 remained uncovered. These rate changes are not explained solely by cold period occurrences, since they are closely correlated to river slope gradients. For the same segments, the river slope increases from 1.7%, to 2.9%, to 2.7%, and to 5.09%. Cold periods and uncovered riffle reaches are however necessary to produce the amount of ice necessary to overcome such slope increases. These initial conditions were not met from PK19 to PK36. Cold periods with strong FDD closely relate to episodes of ice front progression. As the ice cover forms, high flow frazil factories close and low flow areas are converted in undercover frazil accumulation zones (*frazil sinks*).

Finally, a frazil jam occurred at pool section (b) from 12/11 to 12/13. It contributed to a significant increase in water level without precipitations or discharge change. Figure 4b shows a 3-days interruption in frazil/ice fragments inputs at pool section during the frazil jam. Unfortunately our water level loggers did not translate a backflow effect. Massive frazil transits were observed up from 12/14 to 12/22 reflecting intense upstream production and frazil transport to newly formed frazil sinks. The jam is associated to a strong increase in regional FDD.

Evolution of ice and bed morphology

Figure 6 shows January's GPR analysis and February-March's drill-hole measurements results at pool cross-sections (CS). Measurements began after 10 weeks of frazil production. This figure illustrates dramatically the role of frazil ice morphology in small rivers. Results show two ice layer interfaces. First, the bottom of ice accumulation is presented as a roughly linear interface that never exceeds 1 meter in thickness. In comparison, the second interface, bottom of frazil accumulation, is highly asymmetrical and easily grows to considerable depth. Frazil spatial distribution is resumed hereafter:

- Bed entrance slope CS-1: frazil layer rests on a left bank shoal. Main inflow is frazil-free
- Recirculation plateau CS-2, 3, 4: a thin water lens separates the frazil from the bed surface. Distance from bed increases as inclination increases towards the cliff. Interestingly, CS-4 shows a thin recirculation channel clear of frazil along the left bank. The same channel is nearly filled with frazil at CS-3.
- Pool-center CS-2, 3, 4: the frazil layer presents an irregular shape allowing a minimal flow depth of ±2 m towards the cliff which remained frazil-free. CS-3 shows no frazil accumulation at pool-center on 02/29. This can be linked to the air temperature rise.
- Exit-slope CS-5, 6, 7: CS-5 leftward migration of the channel water lens is not surprising for a meander pool where current is typically directed towards outer bank at the bend exit. Surprisingly, CS-6 and 7 show a temporal migration from center to left bank between surveys. CS-7 01/29 and 02/29 frazil layers reflect conventional pool-riffle crossing flow structures.

DBR sensors were designed to reveal the time of occurrence of riverbed deformation during icecover conditions. DBR in-flow sensors FS-1, 2, 3, 5 and 7 maintained constant activity patterns. This shows that near-bed flow conditions near those sensors were not affected by frazil. Exit-slope FS-4 and 6 have been inactive from the end of Nov. to May 18th. This indicates that local flow conditions were reduced. Bed or ice deposition may have jammed the sensors. Ice cover formation has clearly triggered a movement response from non-moving cliff FS-2 and exit-slope FS-6. Below the bed's surface, in-ground sensors GS-7 and 8 also moved in synchronicity with ice cover formation at revealing intense erosion activity at pool center. This suggests that morphological changes at pool center are linked to the formation of an ice cover through rapid water level increase. However, this morphological change is of short duration considering its singular response. Morphological changes were also linked to changes in discharge. Pool-center FS-8 became permanently responsive to flow after Nov. 15th's increasing discharge. GS-4, 6 also responded to this event translating as strong erosional activity at exit-slope.

Bathymetric surveys, channel soundings descriptions, DBR experiment results, serve to evaluate riverbed deformation. Bathymetric surveys comparison shows a 50 cm erosion at the cobble bed entrance slope. DBR-1 measured height confirmed this erosional pattern with a 5 cm erosion of marine clay bed (Fig. 7). Corresponding frazil layer, at pool center CS-2 and 3, reveals flow geometry adapted to maximum velocity current near inner bank at bed-entrance. The right bank also shows strong erosion where meander bend was cut-off at high-flows. Deposition is found at three morphological units: at the clay cliff, at pool center and at exit slope. The cliff's deposition was caused by a large landslide from the cliff itself, which was confirmed during a scuba dive. Unfortunately, DBR-2 in-ground sensor (GS) and in-flow sensor (FS) did not register the event nor did in situ measurements although local bed was composed of fine gravels. The exit-slope deposits correspond to a sandy point bar development.

5. Discussion

Mitis river's frazil supply was continuous throughout the winter owing to the absence of ice cover on steep slope reaches. We believe that the upstream activation of frazil factories continued upstream from PK36 where numerous upstream riffles became late producers. The presence of permanent ice cover openings in riffles suggests the existence of *polyneas* acting as related frazil factories. The infilling at the pool study site happened within 7 weeks of full cover

formation. Frazil layer and ice cover physical attributes have not changed considerably during the following weeks. This implies the future challenge of investigating younger and thinner ice covered conditions.

DBR results show a clear relation between riverbed deformation and ice cover formation. Yet, this relation did not produce enduring changes. On the contrary, the enduring riverbed erosion found at pool center could not be proven ice related. The lateral migration of a water lens at CS-1 suggests a possible local bed deformation, unfortunately DBR were not deployed in this area because of its shallow depth. Inspired by the ice and hydraulics equilibrium concept, we believe that frazil growth is limited by hydraulic and thermal variables resulting in a unique winter hydraulic geometry (Michel and Drouin, 1975). As presented by Shen (1995), frazil granules are subject to shear stress like bed particles. Induced deformation by frazil accumulation should only be found where sediment size resistance to shear stress is lower than frazil resistance. In accordance with this, CS-1 riverbed is mainly composed of sand and silt, a common sediment population for exit-slopes.

6. Conclusions

The infilling dynamic of frazil sink depends on multiple interactions between hydroclimatic parameters and cold river dynamics. Frazil ice production and ice cover formation are presented as they relate in space and time to hydroclimatic conditions and to morphologic features. Innovative methods were developed and tested. Dynamic bed-rods effectively documented the temporality and spatiality of channel response to specific events. Their sensibility to flow strength should be adapted to local flow conditions. Though undoubtedly a complex technology, GPR is usable to detect frazil ice. Frazil ice accumulations in small rivers are surprisingly important and should be regarded as an intrinsic morphological component rather than as punctual localized ice deposits.

References

Ettema R., 2002. Review of alluvial-channel responses to *river ice*. Journal of Cold Regions Engineering, 16(4), 191–217.

Michel, B. and Drouin M., 1975. Equilibrium of a hanging dam at the La Grande River. Rep. GCS-75-03-01, Université Laval, Québec.

Shen, H.T. and Wang, D., 1995. Undercover Transport and Accumulation of Frazil Granules. Journal of Hydraulic Engineering, ASCE, 121 (2), 184-195.

Sui, J., Hicks, F. and Menounos, B., 2006. Observations of riverbed scour under a hanging ice dam. Canadian Journal of Civil Engineering 33: 1-5.

Sui J.Y., Wang D.S. and Karney B.W., 2000. Suspended sediment concentration and deformation of riverbed in a frazil jammed reach. Canadian Journal of Civil Engineering 27 (6): 1120-1129.

Table 1. Summary of methods.

Survey	Specification	Description
Freeze-up survey		
Visual on-site observations	27 survey sites 21 observations	**Iceform classification details** (1) frazil fragments: frazil crystals, ice particles, frazil granules and poorly agglomerated frazil; (2) hydraulic resistant ice aggregates: frazil flocs and floes, floating slush, ice clusters and ice cover fragments all with a minimal surface diameter of 10 cm; (3) anchored ice forms; (4) partial and full ice cover (static and dynamic).
Digital camera	RECONYX Silent ImageTM – Professional, Model PM35 (standard) Passive InfraRed (PIR) motion detector; 100ft, 40° angle field view; 256MB picture resolution; 10 minutes time lapse setting.	
Hydroclimatic data		
Air temperature	Digital temperature loggers iButtons® DS1922L/T from DALLAS Semiconductor.	Air temperature measurements 1.5 meters above ground within 10 meters of river bank. Accuracy of ±0.5°C (8-bit) from -10 to 65°C (0.9°F over 14F° to 149°F).
Water temperature	HOBO® Pro v2 Water Temperature Data Logger from Onset Computer Corporation.	Logger is positioned at a depth of ±1m, ±10cm above river bed. In water accuracy of 0.2°C over 0° to 50°C (0.36°F over 32° to 122°F).
Water level	HOBO® 30-Foot Depth Data Logger U20-001-01.	Logger is positioned ±10 cm above riverbed. Water level range from 0 to 9 m (0 to 30 ft). Accuracy typical error is ± 0.5 cm (0.015 ft). Temperature measurements with same accuracy and range as Pro v2.
Regional climate data	Canada's national climate archives for station Mont-JoliA.	Average temperature, precipitation, freezing degree days (FDD), atmospheric pressure data
Ice and bed morphology		
Bathymetric surveys • 2007 – 1124 sounding • 2008 – 682 sounding	Electronic theodolite Leica TC705 supplies XYZ coordinates. Porro prism was mounted on top of a leveling rod.	Random pole-sounding measurements. Mean Euclidian distance of 13 m. Accuracy error is ± 0.5 m vertically and horizontally due to flow strength.
Ground profiling radar • 400MHz antenna • 900 MHz antenna	GSSI *SIR-3000 system* from Geophysical Survey Sytems Inc, owned by INRS-ÉTÉ	T_Rate : 100 khz Mode : Time GPS : None Scan samples : 2048 Format : 16 bits Range : variable Diel : 3.1 Rate : 32 Scn/unit : 100-200 Gain : auto
GRS analysis		
Matlab	Basic handling Filtering	• Adjust signal position • FIR wavenumber filter high pass • FIR frequency filter low pass • Symlet wavelet sym 4
ArcGIS	Image conversion and line extraction	• Convert ASCII to raster 1x1 cell • Hand draw a polyline • Convert polyline, to raster, to points • Calculate raster coordinates
Data calibration	Signal wave concordance with drill-hole measurements	Snow ±28cm/ns Ice ±17cm/sec Frazil ±5.3 to 6.5 cm/sec Water ±3.3 cm/sec

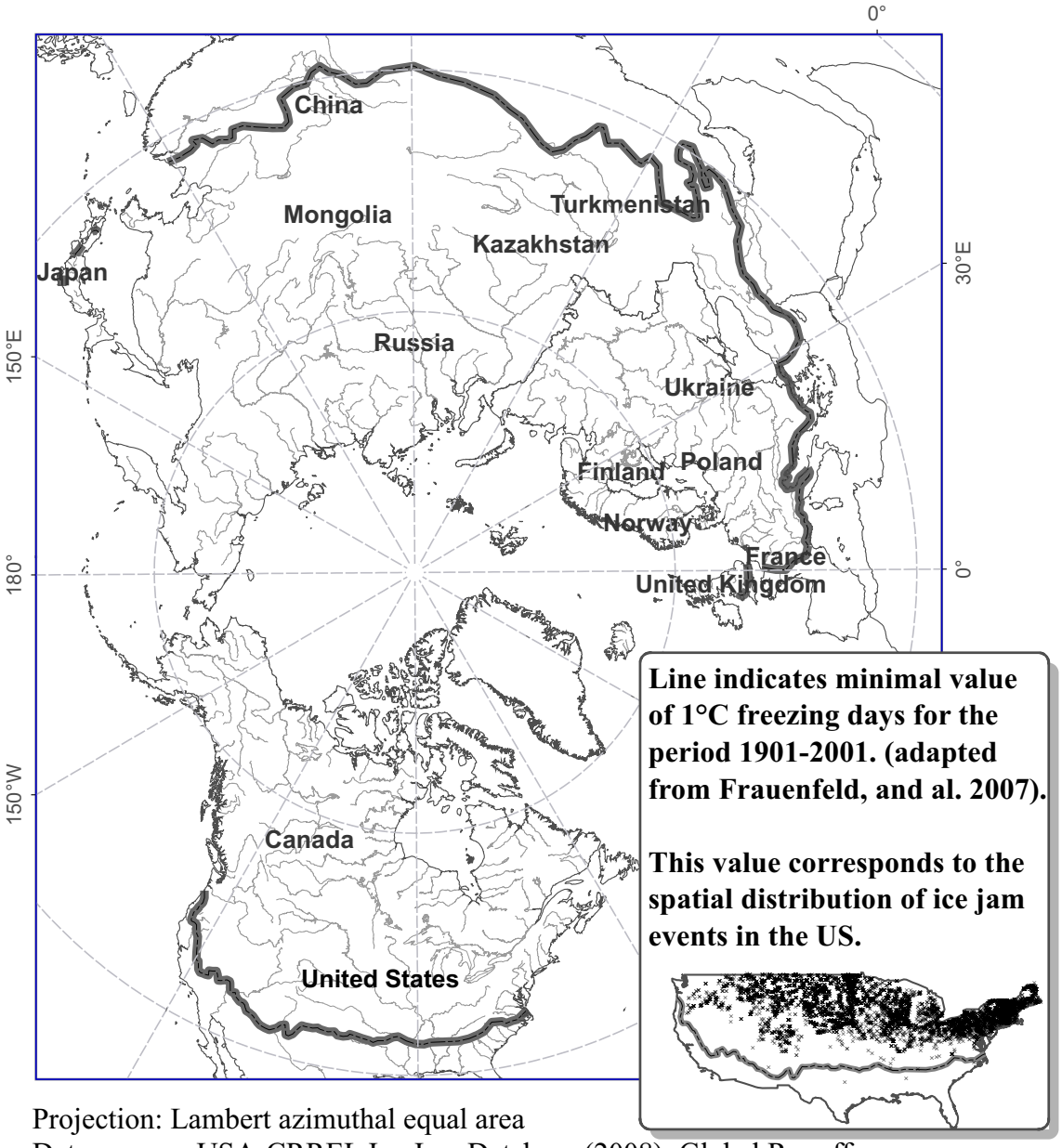

Fig. 1. Cold rivers subject to freezing in the northern hemisphere. Freezing index is based on a continuous long-term 25 km × 25 km grid monthly temperature dataset for the Northern Hemisphere. Monthly dataset is derived from CRU TS 2.1 daily air temperature observations.

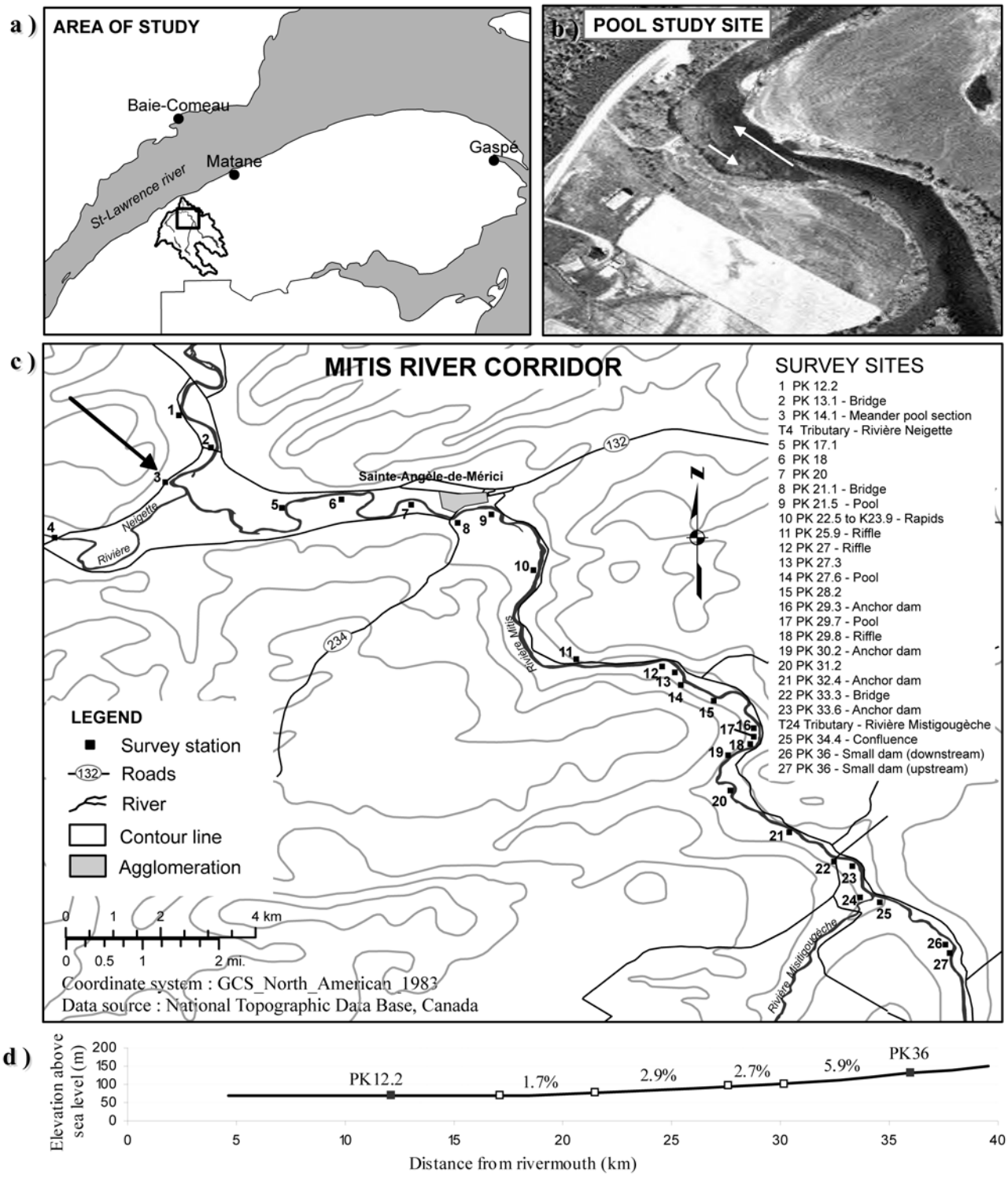

Fig. 2. a) Map showing Mitis river basin and location of Mitis river survey corridor. b) Illustration of the meander pool study site from aerial photograph Q01805-162. rrows indicates flow direction. c) Physiographic map showing freeze-up survey sites along mitis river corridor. The arrow indicates the location of the pool study site. d) Longitudinal profile of the Mitis river corridor.

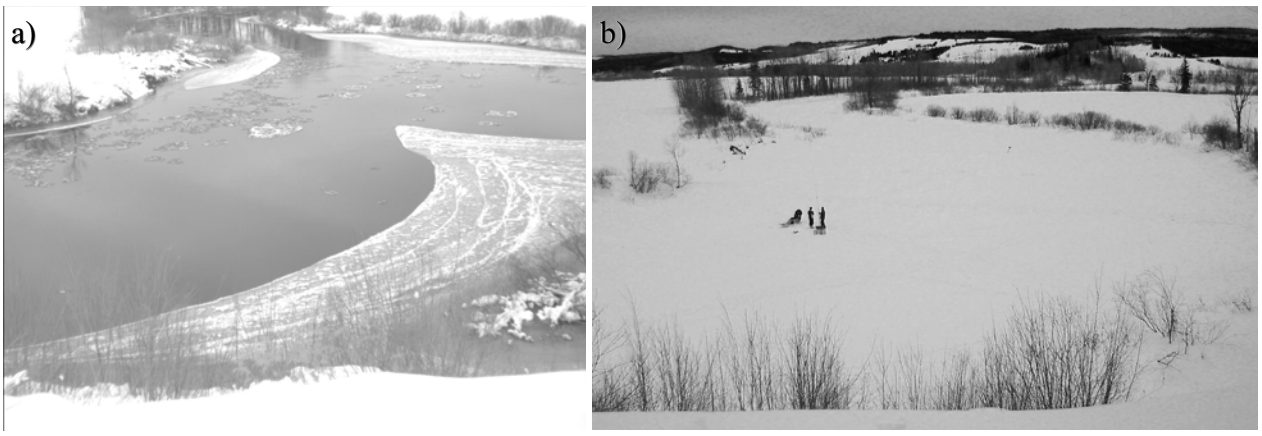

Fig. 3. Southward photos of the study pool area. a) Ice runs on 12/03/2007 at 07h11. b) GPR testing on 03/19/2008.

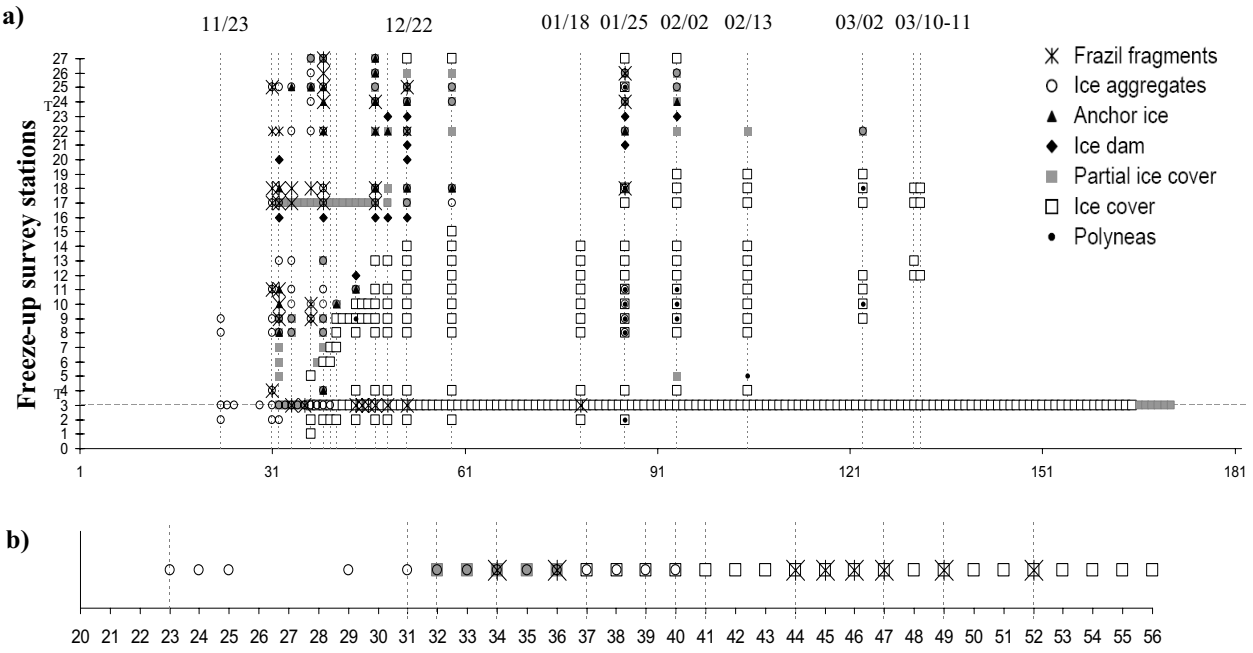

Figure 4. a) Daily hydroclimatic conditions for the period November 1st, 2007 (day 1) to Mai 1st, 2008 (day 183); b) freeze-up at pool section for the period 11/20 to 12/26 (day 56).

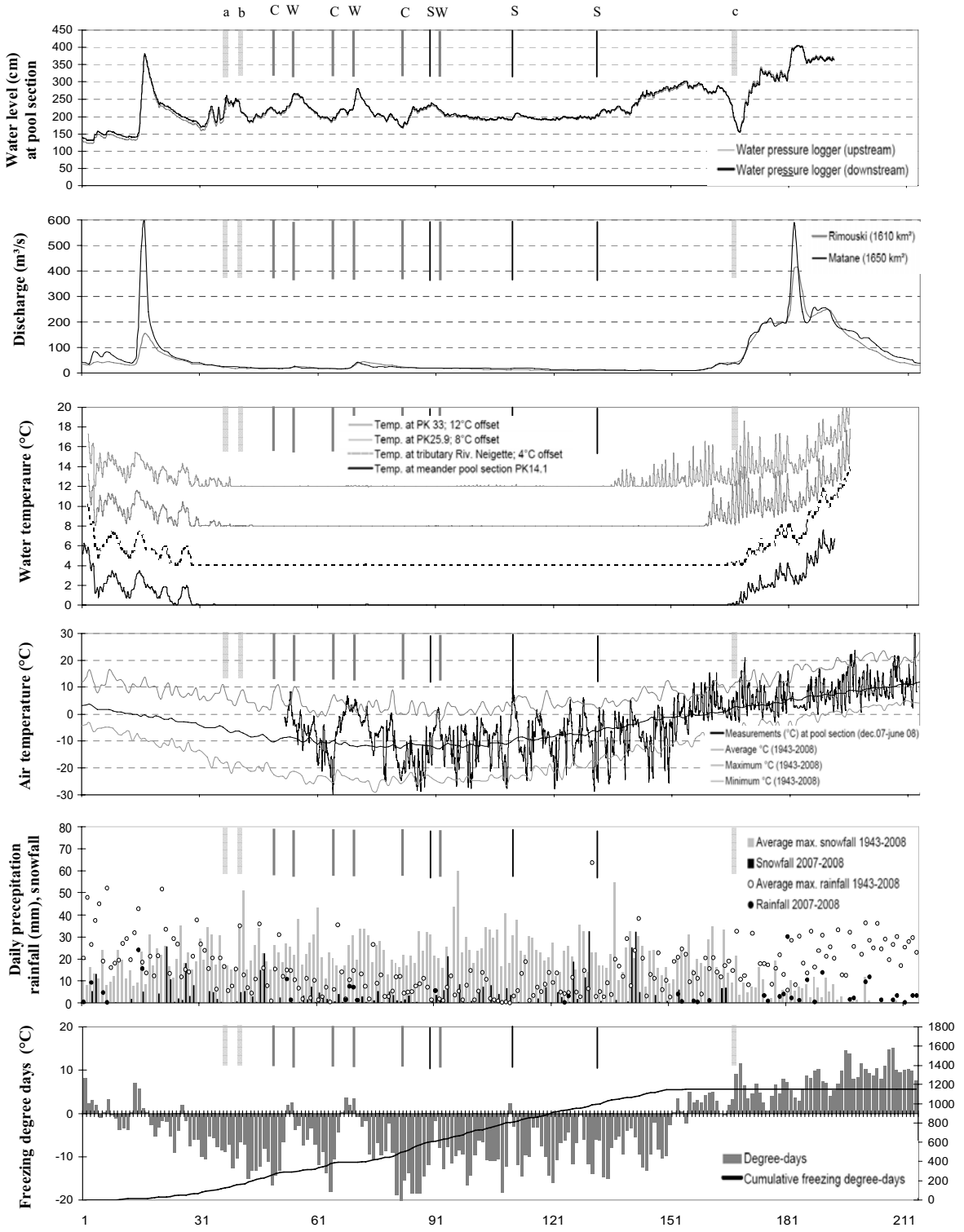

Fig. 5. Daily hydroclimatic conditions for the period November 1st, 2007 (day 1) to June 1st, 2008 (day 214). (a) Ice cover formation 12/07; (b) frazil jam 12/11-13; (c) thermal break-up 04/14; (C) cold periods (12/19, 01/03, 01/21-26) ; (W) warm periods (12/24; 01/09; 01/30); (S) field surveys (GPR 01/29; soundings 02/29 and 03/11).

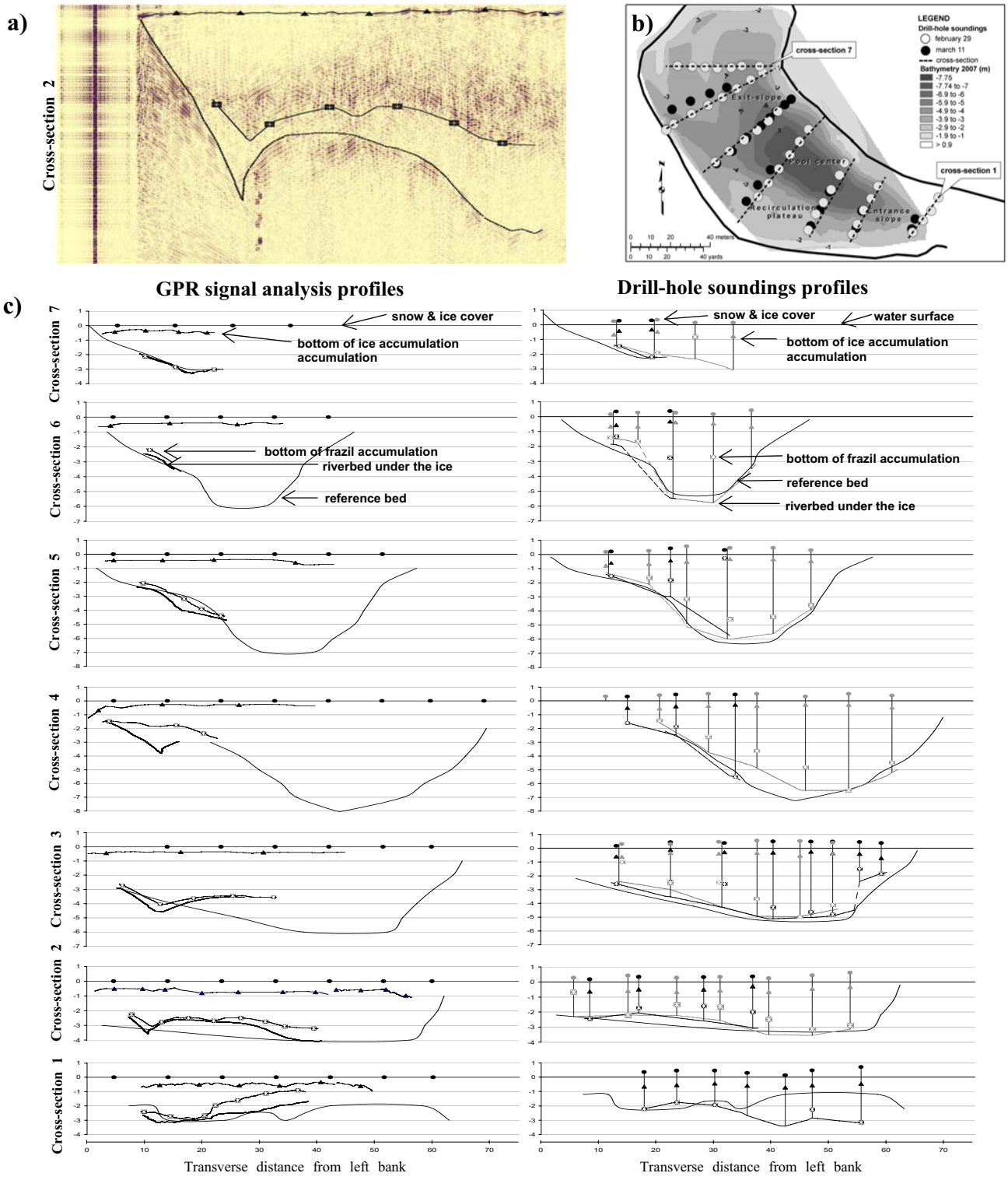

Fig. 6. a) A 400MHz GPR reflection profile after filtering; b) Cross-sections map c) GPR survey analysis cross-sections 01/29 and drill-hole sounding cross-sections 02/29 (black), 03/11 (gray). Cross-section thickness values (m) should be regarded qualitatively.

Accuracy errors: **GPR analysis**: snow signal speed of ±28cm/ns and laminated ice signal speed is not included in snow-ice layer analysis. Frazil layer signal speed of 5.5 cm/ns was calculated for medium dense frazil. This value was applied to all images. Drill-hole soundings revealed that frazil density layers are present and density changes between drill-holes. To accommodate these vertical errors, GPR reference bed was lowered 80cm. **Drill-hole soundings:** measurements have an accuracy error of ± 0.5 m vertically and horizontally due to flow strength.

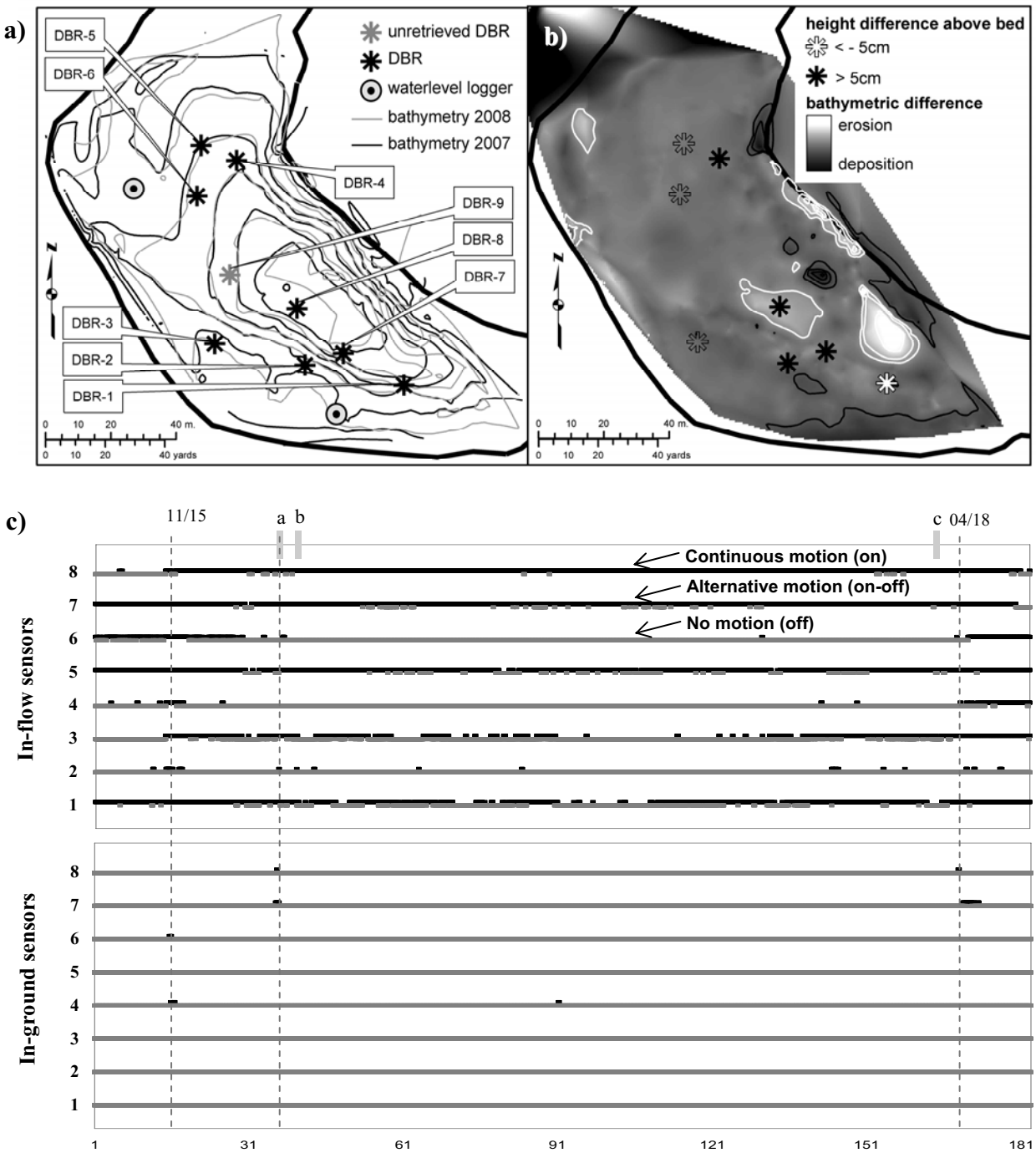

Fig. 7. a) Map showing DBR and waterlevel loggers position at pool site. b) Map showing erosional and depositional activity at pool site. Contour lines indicate 0.5 m elevation difference between bathymetric surveys. White symbols show erosion. Black symbols show deposition. c) Daily on-off acceleration data for the period November 1st, 2007 (day 1) to Mai 1st , 2008 (day 183). Black symbols show the motion position. Gray symbols show the no-motion position. (a) Ice cover formation 12/07; (b) frazil jam 12/11-13; (c) thermal break-up 04/14.